ASSESSMENT OF VOID FRACTION PREDICTION USING THE RETRAN-3D AND CORETRAN-01/VIPRE-02 CODES

Y. Aounallah, P. Coddington

A review of wide-range void fraction correlations against an extensive database has been undertaken to identify the correlations best suited for nuclear safety applications. Only those based on the drift-flux model have been considered. The survey confirmed the application range of the Chexal-Lellouche correlation, and the database was also used to obtain new parameters for the Inoue drift-flux correlation, which was also found suitable. A void fraction validation study has also been undertaken for the codes RETRAN-3D and CORETRAN-01/VIPRE-02 at the assembly and sub-assembly levels. The study showed the impact of the RETRAN-03 user options on the predicted void fraction, and the RETRAN-3D limitation at very low fluid velocity. At the sub-assembly level, CORETRAN-01/VIPRE-02 substantially underestimates the void in regions with low power-to-flow ratios. Otherwise, a generally good predictive performance was obtained with both RETRAN-3D and CORETRAN-01/VIPRE-02.

1 BACKGROUND

In two-phase flows, the liquid/vapour interface can exhibit a wide variety of topological configurations, or flow patterns. These are a consequence of complex interphase exchange mechanisms, which are difficult to capture to a satisfactory level from conservation equations alone. Consequently, much effort has been devoted during these past few decades to develop constitutive equations which can capture some of the complexities of two-phase flows and, consequently, allow the development of tools with good predictive capabilities. Of particular importance in the safety of Light Water Reactors (LWRs) is the void fraction in the reactor core, due to its major impact on neutron moderation, and therefore on power generation and feedback effects. It is also important to determine, for example, the swell level during core uncovery, and the behaviour of other components such as the steam generators in Pressurized Water Reactor (PWR) plants. Moreover, the trend towards best-estimate methodology requires that the models and correlations be assessed more accurately. This article gives a global account of the studies performed, within the framework of the "Simulation Models for the Transient Analysis of Reactors in Switzerland" (STARS) project, to assess the predictive capability of the system code RETRAN-3D [1], and the core and subchannel code CORETRAN-01/VIPRE-02 [2,3].

2 REVIEW OF VOID FRACTION CORRELATIONS[1]

The purpose of this review was to identify the void fraction correlations best suited for nuclear safety analyses - a basic requirement being a broad range of applicability, and the correct asymptotic trends. All correlations surveyed are based on the drift-flux void model, originally developed by Zuber and Findlay [4] and Wallis [5], and formulated as follows:

$$\alpha = \frac{j_g}{C_0 j + v_{gj}} \qquad (1)$$

where α is the void fraction, C_0 and v_{gj} are parameters (experimentally determined) which represent a radial void distribution function and a phase velocity difference, respectively. The variables j and j_g are, respectively, the total and steam superficial velocities.

The evaluation of the drift-flux correlations was based on an experimental database, built to cover a broad range of flow conditions ranging from BWR nominal conditions to a coolant swell-level experiment (PERICLES), a high-conversion-ratio assembly (NEPTUN), and boil-off tests. The database amounted to about 500 data points, obtained from rod bundles, and conducted in nine different test facilities [7-15]. Table 1 gives some basic parameters for these facilities, and complementary information on the range of pressures and mass fluxes covered in these experiments is given in Fig. 1.

Among the 25 drift-flux correlations investigated, those yielding a mean error $\bar{\varepsilon}$, and a standard deviation S larger than 0.10 and 0.15, respectively, were not viewed as suitable for broad-range applications, and were therefore not considered further.

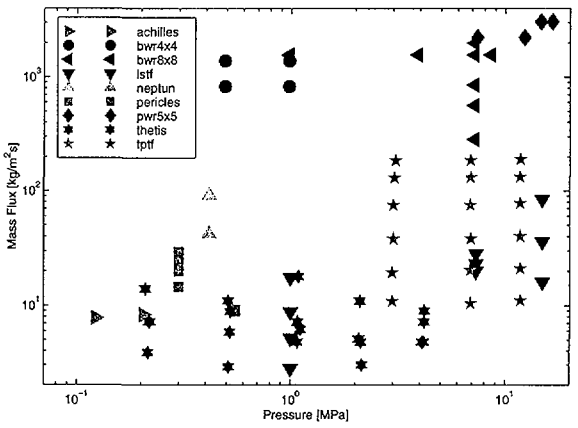

Fig. 1: Range of pressures and mass fluxes covered in the database.

[1] From reference [6]

Table 1: Overview of the experimental facilities and significant parameters (sorted by pressure).

	ACHILLES	THETIS	PERICLES	NEPTUN	BWR4x4	BWR8x8	LSTF	TPTF	THTF
Reference [7-15]	Pearson et al, 1989	Jowitt et al., 1984	Deruaz et al., 1985	Dreier et al., 1988	Mitsutake et al., 1990	Morooka et al., 1991	Anoda et al., 1990	Kumamaru et al., 1994	Anklam et al, 1982
Type	PWR	BWR	PWR	LWHCR[1]	BWR	BWR	PWR	PWR	PWR
L [m]	3.7	3.6	3.7	1.7	3.7	3.7	3.7	3.7	3.7
Rods (heated)	69 (69)	49 (49)	357 (357)	37 (37)	16 (16)	64 (62)	1104 (1008)	32 (24)	64 (60)
d_r [mm]	9.5	12.2	9.5	10.7	12.3	12.3	9.5	9.5	9.5
d_h [mm]	13	13	11	4	12	13	13	10	11
Axial power distribution	chopped cosine	chopped cosine	chopped cosine	chopped cosine	uniform	uniform / chopped cosine	chopped cosine	uniform	uniform
ΔT_{sub} [K]	18/24	25-157	20/60	0.5-3	0*	9-12	0*	5-35	46-118
p [MPa]	0.1/0.2	0.2-4.0	0.3/0.6	0.4	0.5/1.0	1.0-8.6	1.0/7.3/15.0	3.0/6.9/11.8	3.9-8.1
G [kg/m^{2}s]	0.08	2.5-3.1	21-48*	42/91	833/1390	284-1988	2.2-84*	11-189	3.1-29
q [kW/m^2]	11	11/12	11-40	5/10	350-743*	225-3377*	5-45	9-170	11-74

[1] Light Water High Conversion Reactor
* Estimated values

The remaining correlations are listed in Table 2.

In Table 2, the Zuber-Findlay correlation is treated separately, since it formed the foundation for most of the correlations, while the other twelve correlations were divided into three groups. The first group consisted of correlations derived from tube data [16-19].

Table 2: Wide-range void fraction correlations.

Correlation	Year	Data Source	$\bar{\varepsilon}$	s
Zuber-Findlay	1965	Tube	-0.025	0.114
Ishii	1977	Tube	0 048	0.126
Gardner	1980	Tube	0.056	0.111
Liao, Parlos and Griffith	1985	Tube	0.028	0.094
Takeuchi	1992	Tube	0.040	0.083
Sun	1980	RB*+ Tube	-0.041	0.114
Jowitt	1981	RB	0.057	0.116
Sonnenburg	1989	RB + Tube	0.049	0.097
Morooka	1989	RB	0.019	0.103
Dix	1971	RB	-0.010	0.092
Bestion	1985	RB + Tube	0.018	0.088
Chexal-Lellouche	1992	RB + Tube	-0.017	0.078
Inoue	1993	RB	-0.003	0.083
New Correlation	1996	RB	-0.002	0.071

* RB stands for rod bundles

The correlations in the second group [20-22] have a large value for the parameter C_0 in Eq. 1, causing the void to have a maximum $\alpha_{max} < 1$, as does the Zuber-Findlay correlation. The third group [23-26] contains the correlations which gave good predictions over the whole range of void fractions. In this group, the correlations yielded a mean deviation from the experimental data ranging from -0.003 to +0.018, with a maximum standard deviation of 0.092.

The conclusion of this assessment is that, among the many drift-flux correlations available in the literature, the Chexal-Lellouche correlation [25], which has been implemented in RETRAN-3D, is among the most reliable. The study has confirmed the validity of this correlation for a range of operating conditions pertaining to safety analysis. It has also shown that simpler formulations give as good, if not better, results in certain cases.

Furthermore, the database used to assess the drift-flux void correlations was also used to develop a new correlation [6], based on the Inoue drift-flux formulation [26]. (The Inoue formulation itself is based originally on the Dix drift-flux correlation, but with the addition of a pressure dependency in the distribution parameter C_0). The parameters C_0 and v_{gj} in Eq. 1 are expressed as follows:

$$C_0 = C_1 \cdot P + C_2$$

$$v_{gj} = \left(v_1 \cdot P^2 + v_2 \cdot P + v_3\right) \cdot G + \left(v_4 \cdot P^2 + v_5 \cdot P + v_6\right)$$

in which the new coefficients C_i and ν_i, obtained by a least-square fit from the selected database, are given by:

$C_1 = 2.57\text{x}10^{-3}$ $\quad C_2 = 1.0062$

$\nu_1 = 6.73\text{x}10^{-7}$ $\quad \nu_4 = 5.63\text{x}10^{-3}$

$\nu_2 = -8.81\text{x}10^{-5}$ $\quad \nu_5 = -1.23\text{x}10^{-1}$

$\nu_3 = 1.05\text{x}10^{-3}$ $\quad \nu_6 = 8.00\text{x}10^{-1}$

With these adaptations, the standard deviation was reduced from 0.083 to 0.071, with a mean deviation of 0.002 instead of 0.003 compared with Inoue's correlation. Figures 2 and 3 show the system pressure dependency.

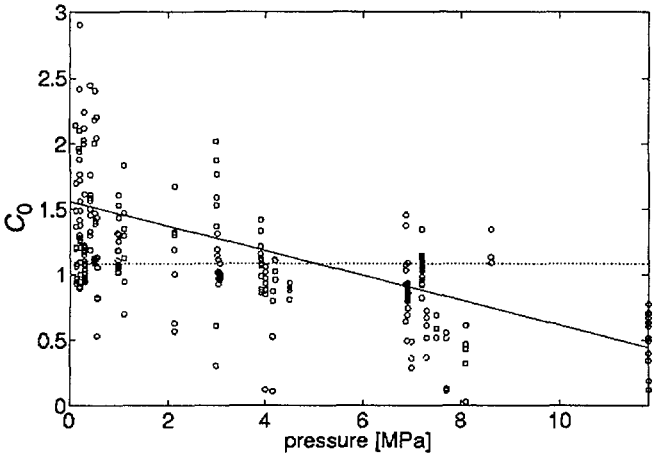

Fig. 2: Effect of system pressure on C_0 with ν_{gj} as parameter.

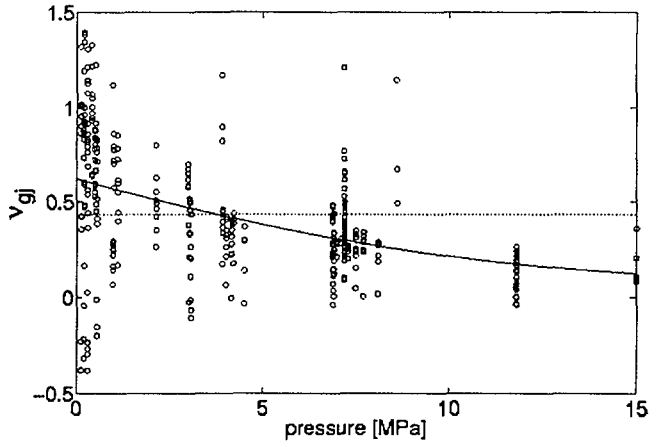

Fig. 3: Effect of system pressure on ν_{gj} with C_0 as parameter.

3 THERMAL-HYDRAULIC CODES ASSESSED

In calculating the void fraction, and other flow quantities, thermal-hydraulic codes often provide several user options which, besides the nodalization and time step selection, can impact substantially on the results. This multiplicity of options stems primarily from the choice of constitutive equations needed to solve the system of (mass, momentum, and energy) conservation equations. Also, depending on the level of complexity and refinements in modelling the two-phase flow, the number of conservation equations can vary from three, for the so-called homogeneous model, to nine in the case of a two-fluid, three-field model - although for practical purposes this number has been limited to seven (e.g. in MONA). Also, while increasing complexity does offer the capability of capturing phenomena which would otherwise not be modelled, it does require an increasing number of closure relations, which then have to be validated for the application at hand. The modelling options are outlined here for the system code RETRAN-3D, and for the core and subchannel code CORETRAN-01/VIPRE-02.

3.1 RETRAN-3D

RETRAN-3D [1], among the family of system codes, has a large number of models. This is partly because, as the code evolved, the models from previous code versions were kept for maintaining the (USNRC) licensed-code capability for a particular version of the code (currently RETRAN-02 MOD005.2), while new models are added in the framework of improving and extending the range of applicability of the code.

Hence, in calculating the void fraction, several options are available to the user, as, for example, for determining the liquid/vapour slip velocity. In the 3-equation option, the code solves the three conservation equations (mass, momentum and energy), and uses a drift-flux correlation to determine the "slip velocity" (i.e., the difference between the steam and liquid velocities), as opposed to the more commonly used "slip ratio". Two drift-flux correlations are available, namely Chexal-Lellouche and Lellouche-Zollotar, while the 4-equation model includes options for the interphase friction factor (e.g. based on a flow-regime map).

In the 4-equation model, the code solves an additional momentum equation to determine the slip velocity. However, both the 3- and 4-equation models are based on thermal equilibrium, and so cannot model subcooled boiling without a special provision to address this limitation. The 5-equation model alleviates the difficulty by adding another conservation equation for the vapour mass, thus allowing the two phases to be in thermal non-equilibrium (the steam still being assumed to remain at saturation temperature), and therefore void formation in conditions of bulk subcooling is then possible.

3.2 CORETRAN-01/VIPRE-02

The VIPRE-02 [3] code has two areas of application: firstly, it can be used as a stand-alone code for subchannel analyses and, secondly, it can be used, coupled to the neutronic module ARROTTA, within the code package CORETRAN-01 [2], which has been developed for detailed, three-dimensional, steady-state and transient core analyses of LWRs.

VIPRE-02 is a two-fluid code, developed to address modelling limitations such as thermal non-equilibrium, inherent to simpler models on which the original version of the code VIPRE-01 [27] was based. VIPRE-02 has two options for the prediction of void fraction, in addition to the so-called homogeneous equilibrium model option. One is based on a flow-regime map (FMAP), while the other is based on the so-called dynamic flow regime model (DFRM). The latter, a 14-parameter model, is one of the most mechanistic models implemented in a thermal-hydraulics code.

While VIPRE-01 has been extensively validated, VIPRE-02 has prompted few validation studies. An assessment of VIPRE-02 has thus been undertaken, due to the importance of the void feedback and therefore power generation, if the code is used within CORETRAN, and also for detailed void distributions which can be significant for accurate steady-state pin power calculations.

4 EVALUATION OF RETRAN-3D SLIP OPTIONS[2]

4.1 Experimental database and code model

The database used for the evaluation of the drift-flux correlations [6] was also used to assess the RETRAN-3D slip options [28, 29]. The test sections in the experiments were simulated in the code using a single channel, comprising typically 25 axial nodes, a fill junction at the bottom to impose the flowrate and subcooling, and a time-dependent volume for the top node to impose the system pressure, as shown in Fig. 4. Core conductors were used to simulate the heater rods and power input. The code was run in steady-state mode for most simulations, but also in the transient mode for the boil-off experiments, for example.

4.2 Comparisons between predicted and experimental results

4.2.1 BWR operating pressure

All the slip options available in RETRAN-3D could accurately predict the void fraction for those experiments which remained close to the normal operating conditions in a BWR core. With decreasing mass fluxes, the measured data was increasingly overpredicted by the Lellouche-Zollotar [30] options, and by the flow-regime-dependent dynamic slip option (Fig. 5).

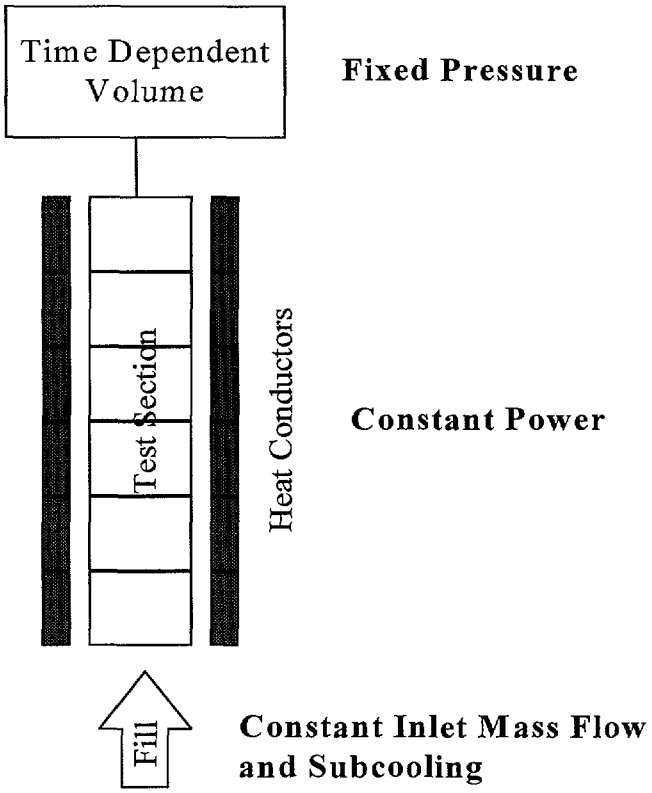

Fig. 4: RETRAN nodalization diagram.

The Chexal-Lellouche option, used in either the three- or four-equation model, can adequately predict the void at low mass flows. At very low flow (less than 50 kg/m²s), and low pressure (less than 20 bar), Chexal-Lellouche drift-flux options significantly overpredict the void. This trend was corroborated by comparisons against experimental data obtained from different test facilities.

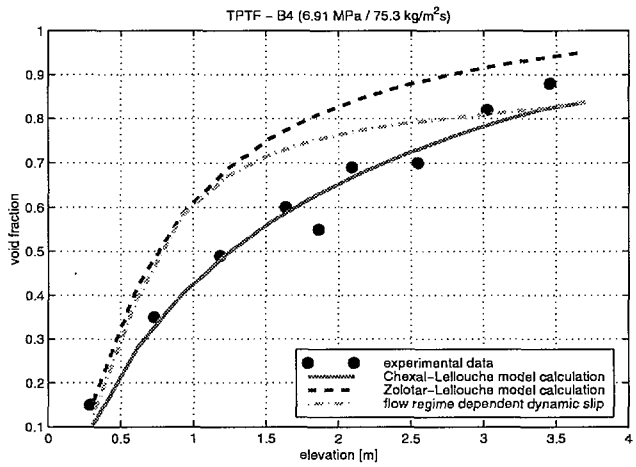

Fig. 5: Prediction of a TPTF experiment using the 4-equation model option.

[2] From references [28, 29]

4.2.2 Very low pressures and flows conditions

The low-pressure/low-flow experiments, such as THETIS, PERICLES and ACHILLES, were difficult to simulate due to code initialisation failure. This was circumvented, in several cases, by initialising the model at a higher flowrate, and then performing a "ramping" from the initial flow conditions to the desired experimental values. However, at pressures below 3 bar, and flows less than 10 kg/m^{2}s, even this method failed, and the code could not be brought to a converged state.

Figure 6 shows the transient results for the collapsed water level in a THETIS experiment performed at 20 bar.

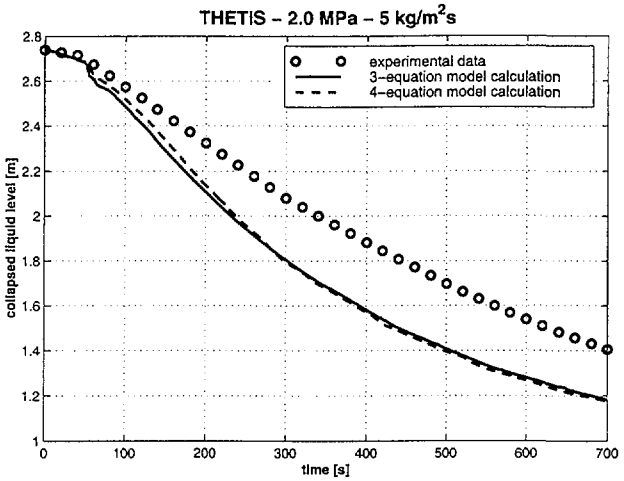

Fig. 6: Prediction of a THETIS transient experiment using the Chexal-Lellouche models.

4.2.3 Very high pressure conditions

Based on the limited amount of data available for very high pressures (greater than 150 bar), with low mass flows, it appears that the Chexal-Lellouche and the flow-regime-dependent slip options significantly underpredict the experimental data (Fig. 7). For these conditions, the Lellouche-Zollotar correlation produces the most accurate results

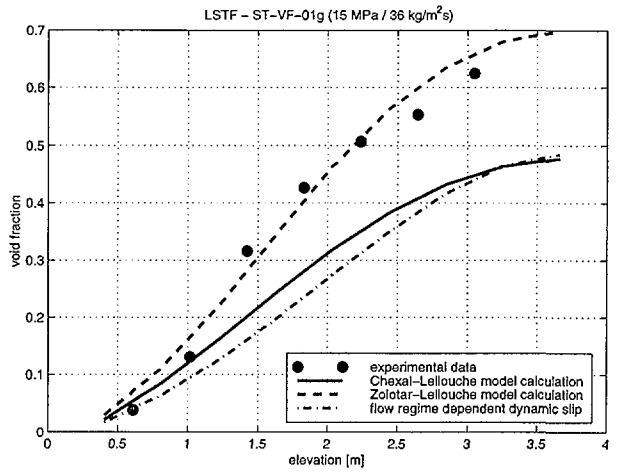

Fig. 7: Prediction of an LSTF experiment using the 4-eq. model option.

4.2.4 Overall results

A comparison of the RETRAN-3D data predictions against the measured void fraction is given in Fig. 8. The calculated void fraction was obtained using the RETRAN-3D 4-equation (dynamic slip) model with the Chexal-Lellouche void correlation, since this provides the most accurate prediction over the widest possible range of parameters. The Figure excludes comparisons against the very low pressure (lower than 3 bar) and low-flow (lower than 10 kg/m^{2}s) experiments, which could not be properly simulated. The database was then reduced to 413 points, with a mean error of -0.008, and a standard deviation of 0.071. In addition, the data at very high pressures, identified with a hollow symbol, show some underprediction. For the intermediate-to-low pressure range, with low flows (e.g., LSTF, NEPTUN and THETIS), there is a consistent overprediction.

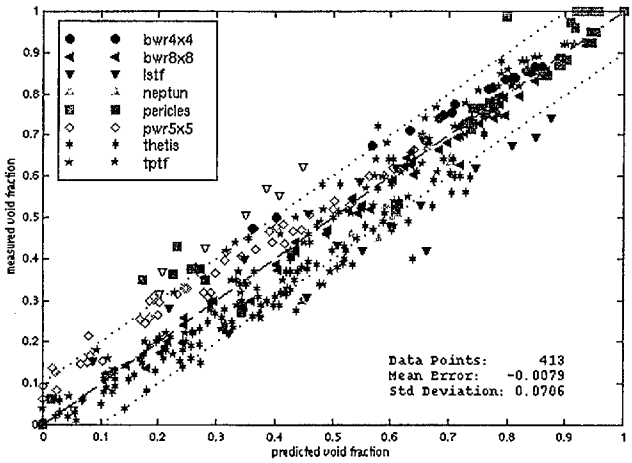

Fig. 8: Overall comparison of predicted and experimental data.

To summarise, several observations can be made with a high level of confidence. For conditions which remain close to BWR operating conditions, all the slip options available in RETRAN-3D give good results. With decreasing flowrates, the void is increasingly overpredicted. At very low pressure and low flows (less than 3 bar and 10 kg/m^{2}s), RETRAN-3D either fails to converge or exhibits artificial oscillations. At very high pressures and low flows, the flow-regime-dependent slip options significantly underpredict the experimental data. For these conditions, the Chexal-Zollotar option gives the best results.

5 ASSESSMENT OF THE SUBCOOLED VOID PREDICTION[3]

5.1 NUPEC experiments and code modelling

Because the early void fraction data were not directly measured, but inferred from pressure drop measurements, the need for more accurate data has spurred new efforts. Unfortunately, such data are usually not publicly available. However, NUPEC (Nuclear Power Corporation - Japan) has published void fraction data

[3] From reference [31]

obtained by applying X-ray and CT-scan techniques. This smaller, but more reliable, database [32-34] has been used to assess the subcooled boiling models in RETRAN-3D and VIPRE-02, as well as the subchannel saturated void model in VIPRE-02 (see Section 6).

For the subcooled boiling experiments, the NUPEC test section consisted of a 5x5 array of full-length rods (effective heated length 3.66 m), simulating a section of a Japanese 17x17 PWR fuel assembly. The fuel rods were simulated by electrically-heated Inconel-600 tubes; the rod diameter was 9.5 mm and the rod pitch 12.6 mm. Tests were performed with both uniform (Bundle A) and chopped-cosine (Bundles B and C) axial profiles. Bundle C, not shown here, included one unheated rod. The void fraction was measured at fixed locations along the heated length, using X- or gamma-ray attenuation techniques, and with a CT scan at the channel exit. The void was given as a function of the (cross-section-averaged) thermodynamic quality. The (PWR) subcooled void data were given in the form of bundle-averaged void versus thermodynamic quality.

5.2 Comparisons between experimental and code results: rod bundle tests

The comparison in this section also includes results from the TRAC-BF1 code.

5.2.1 Pressure 74 bar

Figure 9 shows the results for the lowest pressure of 74 bar, typical of BWR normal operation. With the exception of the RETRAN-3D 5-equation model, the calculated and experimental data all show a similar point of net vapour generation (the slight discontinuity in the slope is caused by the axial nodalization). The calculated results can be divided into three groups, with the calculations from the two profile-fit (or pf) models, i.e. TRAC-BF1 and RETRAN-3D (pf), producing very similar results. The RETRAN-3D (5-eq.) model produces the largest void fraction (in the subcooled region), while VIPRE-02 produces the smallest. We also see that TRAC-BF1 and RETRAN-3D (pf) give the closest agreement with experimental data. The largest difference is that between RETRAN-3D (5-eq.) and VIPRE-02, even though both codes are based on the same underlying model [34].

5.2.2 Pressure 123 bar

The experimental data shown in Fig 10 were obtained from Bundle A, which has a uniform axial power profile. It should be noted that, in contrast to the results in Fig. 9, the lowest quality data came from the measurement station located just above the test section mid-plane and, under these conditions, the heat flux in Bundle B is higher than that in Bundle A.
The most noticeable difference between the calculated results is the point of net vapour generation. For the TRAC-BF1 calculation, which is based on the Saha-Zuber correlation, the higher heat flux at the point of net vapour generation in Bundle B (Fig. 9) explains why this point occurs at a lower quality. In general, in the subcooled region, for which there is a higher heat flux, i.e. Bundle B, the experimental and calculated results show a higher void fraction for a given quality.

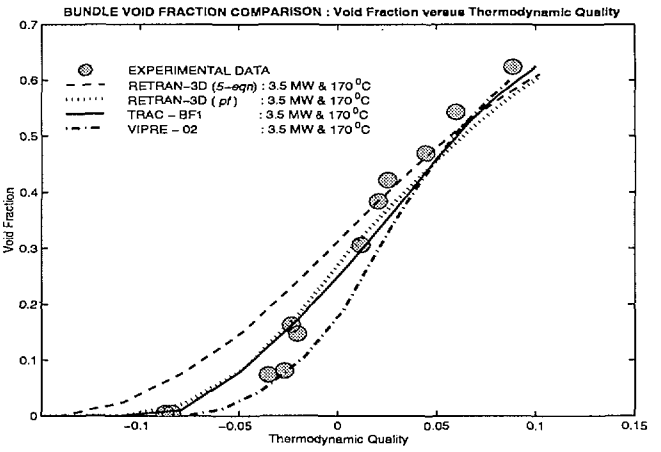

Fig. 9: Rod Bundle B comparison, pressure 7.4Mpa.

This is because, the higher the heat flux, the greater the proportion which goes into vapour production. In the subcooled region, there is a tendency to over-predict the experimental data. For qualities higher than 0.05, both phases are in thermal equilibrium, and all codes show an underprediction of the data.

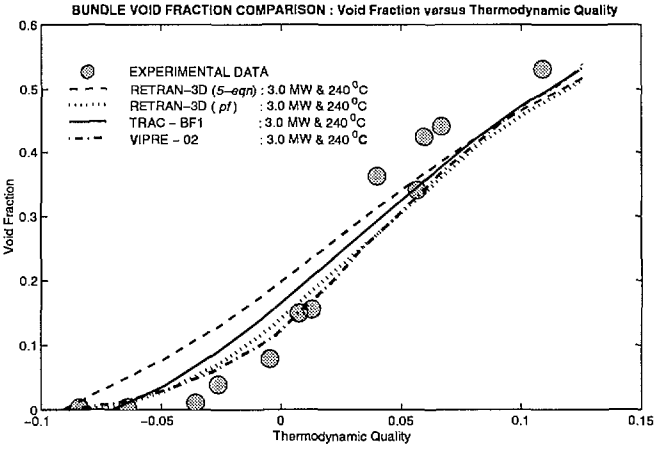

Fig. 10: Rod Bundle A comparison, pressure 12.3 Mpa.

5.2.3 Pressure 147 and 166 bar

The data at 147 and 166 bar were obtained from Bundles A and B, respectively. Figure 11 shows the impact of combinations of heat flux and inlet temperatures on the results. As expected, the void fraction increases with heat flux, for a given quality, while variations in the inlet temperature produce almost no observable difference, because of the high inlet subcooling.

At these high pressures, all codes predict that (i) the point of net vapour generation is at too low a value of the equilibrium quality, and (ii) the rate of increase in void versus quality is severely underpredicted. Consequently, although the point of net vapour generation is predicted too "soon", the void is still underpredicted in the saturated region.

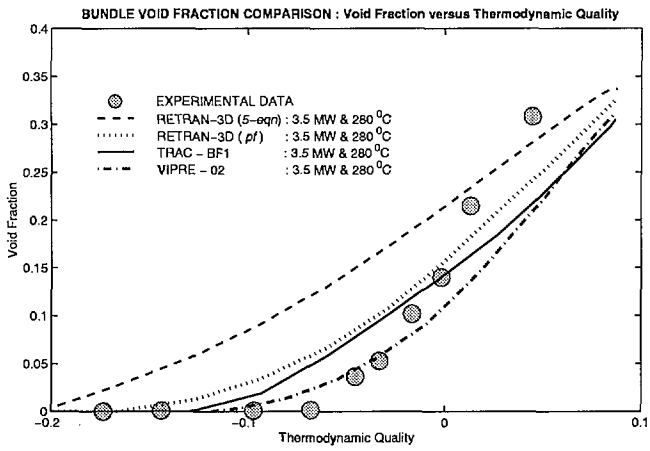

Fig. 11: Rod Bundle B comparison, pressure 166 bar.

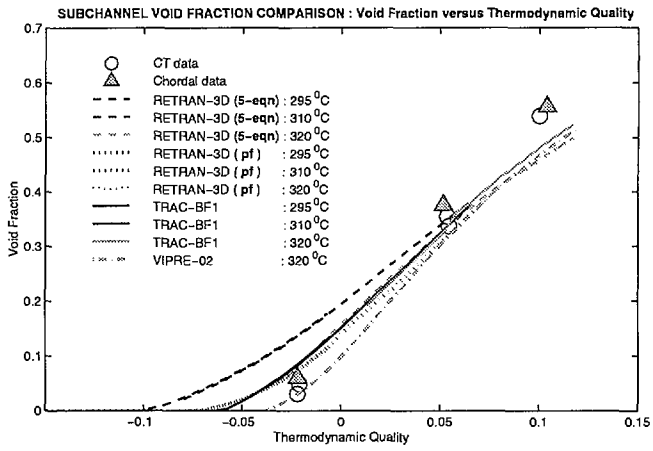

Fig. 12: Subchannel comparison, pressure 123 bar.

5.3 Comparisons between experimental and code results: single subchannel tests

A series of single subchannel experiments, covering pressures ranging from 49 to 166 bar, were also conducted by NUPEC. Here, the void fraction was measured only near the top of the test section, but using two different techniques: a CT-scan and a gamma-ray attenuation technique (chordal data). In these tests, the point of net vapour generation could not be identified. However, the ranges of pressure, heat and mass flux were slightly wider than those for the rod bundle experiments.

For the pressure range between 49 and 74 bar, covering different combinations of heat and mass flux, the agreement between the calculated and measured data is generally very good. This is to be expected, since the majority of the previously available data used to develop these models were from pressures between 50 and 70 bar. However, as for the rod bundle data, the RETRAN-3D (5-eq.) model consistently produces higher voids in the subcooled region.

At 98 bar, the agreement is similar to that at lower pressures, also for a combination of heat and mass fluxes (123 bar to 166 bar), with good agreement for positive qualities.

There is a consistent overprediction of void by the RETRAN-3D 5-equation option at low and negative qualities. All code calculations tended to underestimate the void at high qualities.

In the high pressure range, i.e. from 123 to 166 bar, all the codes show trends similar to those obtained for the rod bundle data: i.e., all tended to underestimate the void at high qualities, and in particular the calculated void fraction increase as a function of quality was smaller than that from the experimental data. Figure 12 gives an example of the results at 123 bar.

All the tests show that the rod bundle and the subchannel results are consistent. The subcooled void tends to be overpredicted, while the saturated void tends to be underpredicted.

6 ASSESSMENT OF SUBCHANNEL SATURATED VOID PREDICTION[4]

6.1 The NUPEC experiments and code modelling

A literature survey has revealed that *subchannel* void fraction measurements which are non-proprietary, and which lend themselves to code validation, are scarce. Among the experimental results published to date by NUPEC, void fraction data are available for full-scale BWR assemblies, mostly under normal operating conditions. Results for three types of assemblies have been reported: the standard BWR 8x8, the so-called "high burn-up" assembly (comparable to a GE-9 and GE-10), and a BWR 8x8 with part-length rods. The rods were electrically heated with local peaking factors typical of BWR configurations. Prototypic spacers were used in all test sections.

The void fraction was measured at fixed locations along the heated length, using X-ray or gamma-ray attenuation techniques, together with a CT-scan at the channel exit. The bundle-averaged and sub-assembly (or regional) void distributions are given, but not the actual subchannel data. These regions represents five concentric rings: a central region (CENTR), a peripheral region (PERIF), and three intermediate regions (INER1, INER2 and INER3), as shown in Fig. 13. In the experiments, the pressure ranged from 39 to 86 bar, and the flowrate from 284 to 1988 kg/m^{2}s. VIPRE-02, being a versatile subchannel code, was able to simulate all features of the experiments.

6.2 Comparisons between NUPEC and code results

In a first stage, the code default options were used for the *base* cases and then sensitivity tests were performed. As with the published NUPEC studies, the results are shown here using two types of plots: (a) bundle-averaged versus equilibrium quality, and (b) subchannel, or regional, void distribution at a given equilibrium quality. The qualities correspond to flow regimes ranging from bubbly to early-annular flow (i.e. from x=0.05 to 0.2 approximately).

[4] From references [35, 36]

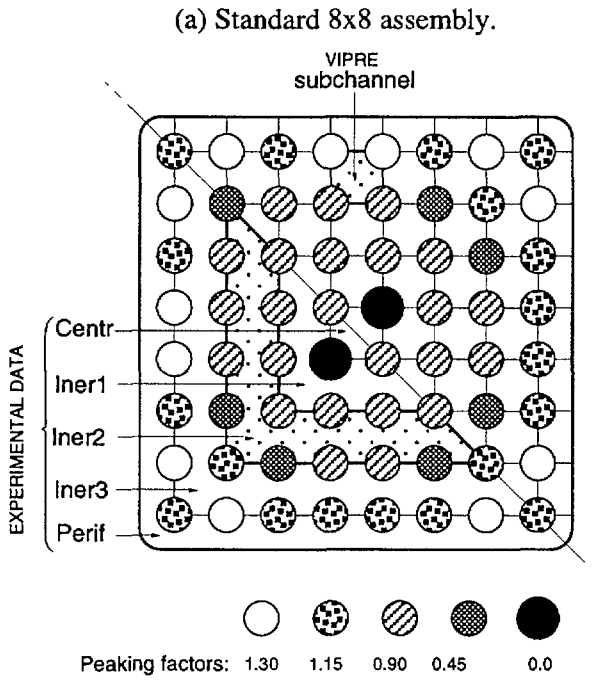

Fig. 13: Subchannel configuration.

6.2.1 BWR nominal conditions

For BWR nominal conditions, both region-averaged and bundle-averaged data are available for comparison. VIPRE-02 systematically overpredits the bundle-averaged void fraction by about 0.04 (Fig. 14).

For the "high burn-up" assemblies, the discrepancy increases somewhat due to the presence of the large central water rod, causing a void depression over a relatively large flow area. The unpowered rod impact can be seen from the sub-assembly, or regional, results shown in Fig. 15.

The subassembly plots indicate an underprediction in the vicinity of the water rods, as shown in Fig. 15. This is attributed to the lack of a lateral void migration model. This void *drift* phenomenon is described in Lahey and Moody [42] as a "strong tendency of the two-phase system to approach an equilibrium phase distribution", and is implemented therein on the basis of an equal-volume exchange between adjacent channels, as opposed to an equal-mass exchange, as implemented in VIPRE-02.

Another feature not modelled in VIPRE is the droplet field in the annular flow regime.

This third field is important when modelling the impact of the spacers on the void fraction and dryout conditions. For the work reported here, this code limitation does not undermine the validation, since only a small fraction of the data available would correspond to the annular flow regime. Apart from nominal conditions, the influence of several parameter variations has been considered, as reported below.

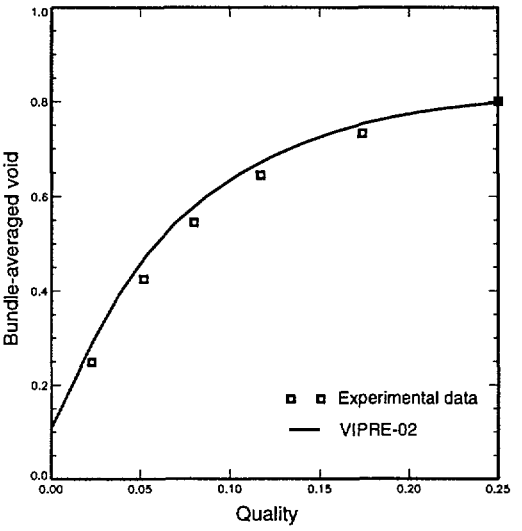

Fig. 14: Bundle-averaged void versus equilibrium quality: BWR nominal conditions.

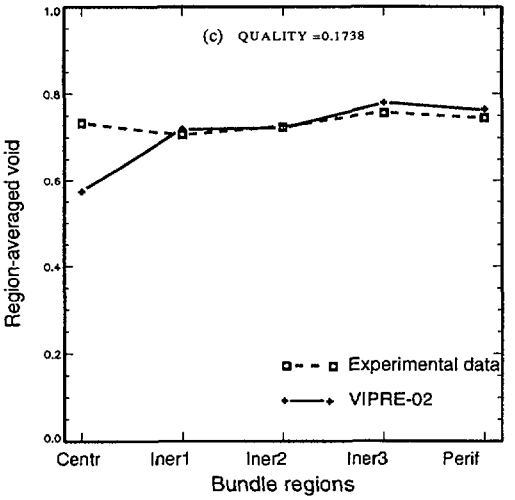

Fig. 15: Region-averaged void for the standard 8x8 assembly: BWR nominal conditions.

6.2.2 Mass flux

Bundle-averaged void data obtained for mass fluxes ranging from 284 to 1988 kg/m^{2}s are reported (representing variations from 20 to 130% of nominal conditions). The experimentally observed effect of reducing the flowrate is to reduce the void fraction for a given quality. The code reproduces this effect, which can be explained by recognising that a decrease in the flowrate increases the slip ratio. Moreover, the magnitude of the effect is also flow-regime dependent, with maximum impact occurring at a quality of about 0.05.

Towards the low-quality region, bubbles tend to be smaller, and to be entrained at a velocity close to the bulk velocity, thus reducing the slip, and therefore the flowrate effect. At high quality, the annular flow regime develops, and the trend is reversed. The flowrate effect decreases again as the slip is primarily controlled by the vapour velocity, while the liquid is now concentrated in the slow-moving film at the wall (there is only a little liquid entrainment at this stage).

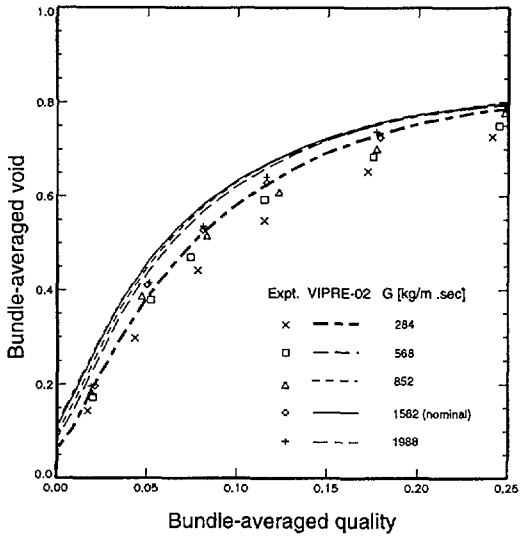

Fig. 16: Bundle-averaged void versus quality: mass flux parameter.

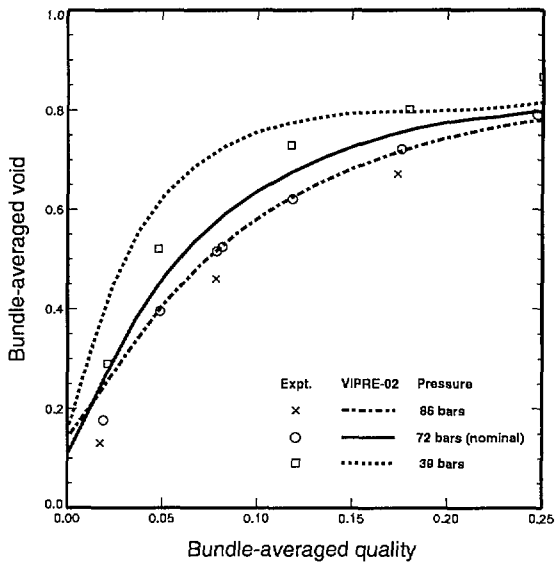

Fig. 17: Bundle-averaged void versus quality: pressure parameter.

6.2.3 System pressure

Experimental void-fraction data were obtained at system pressures of 39, 72, and 86 bar, as shown in Fig. 17. The increase in system pressure decreases the void fraction, primarily as a consequence of the decrease in density ratio. Here again, VIPRE-02 systematically overpredicts the void, except for the case of lowest pressure and highest quality, where the void profile seems to have reached a plateau. This plateau occurs at a void fraction of about 0.8, which is the value usually accepted for the development of the annular flow regime.

Hence, the code underprediction is consistent with the lack of a droplet field in the annular flow regime in which the droplets travel at a higher velocity than the liquid film at the wall. The mean liquid velocity would then be increased, thus reducing the slip and increasing the void fraction.

6.2.4 Part-length rods

The effect of part-length rods on the void distribution has also been investigated by NUPEC for two modified 8x8 assemblies. In these assemblies, the water rods were truncated to an elevation 50 mm below the CT scan measurement level for Assembly No. 5, and 600 mm for Assembly No. 6. The experimental regional results, with and without part-length rods, could not be compared because the published data were given at different equilibrium qualities.

However, the effect was reported to be small, and the code gave the correct trend: i.e. an increase of 0.05 in the void fraction for the central region, and practically no impact on the surrounding regions, as shown in Fig. 18 for Assembly No. 5. The results for Assembly No. 6, not shown here, are similar. In addition to the lack of a void drift model in VIPRE-02, as in most subchannel codes, the cross-flow loses its directional identity once it crosses the subchannel lateral gaps, and therefore does not directly affect the cross-flow in the neighbouring subchannels.

Consequently, the net cross-flow downstream of the truncated rods may not be adequately accounted for by the code. As these flows originate from regions with relatively high void content, they would contribute substantially to the increase of the void in this region.

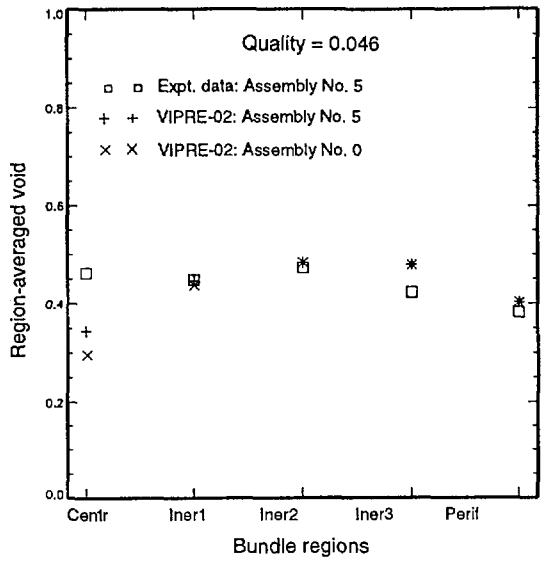

Fig. 18: Region-averaged void: part-length assembly.

6.2.5 Sensitivity calculations to code options

These calculations were aimed at identifying which code-user options could influence substantially the void fraction results. The calculations performed include sensitivity to:

- boundary conditions (i.e. an inlet flowrate versus a total-pressure-drop boundary condition);
- empirical parameters in the enthalpy mixing models;
- nodal pressure, as opposed to the system pressure, for evaluating the fluid thermodynamic properties; and

- void model option, i.e. using the Dynamic Flow Regime Model (DFRM), as opposed to the more standard flow-regime-based (FMAP) void model.

The outcome of these calculations was that only the void model option yielded significant differences. The DFRM option uses one of the most mechanistic two-fluid models available to date. However, scoping tests have shown that predictions were not as good as those obtained using the standard option, and that further effort would be required to adequately assess the full potential of this 14-parameter model.

In conclusion, the main discrepancy between the measured and calculated void fractions is for assemblies exhibiting large variations in power-to-flow ratios, or those containing water rods. This is attributed to the lack of a lateral-void drift model in VIPRE-02. While this effect is negligible for the standard 8x8 assembly, when considering the bundle-average void, it can become appreciable for newer assembly designs with large central water rods.

Also, the lack of models for estimating the effect of the spacer grids on the (i) local mixing, (ii) acceleration pressure drop, and (iii) entrainment in the annular flow regime, should also to be mentioned.

7 CONCLUSIONS

Several conclusions can be drawn from the studies. Among the several drift-flux void correlations reviewed and assessed against a wide range of experimental data, the correlation used in RETRAN-3D, the Chexal-Lellouche correlation, was among the (four) best correlations, and yielded a standard deviation S=0.078, with a mean m=-0.017. These values are larger than those obtained using Chexal-Lellouche, i.e. S=0.049 and m=-0.004, in the study with their own database. A new set of parameters for the Inoue formulation was developed using the current database, and a standard deviation of S=0.07 was obtained, with a mean of m=-0.02.

A systematic evaluation of the slip options available in RETRAN-3D has shown that all the options provide good prediction of the experimental data for pressures and mass fluxes typical of normal BWR operating conditions. However, there is a progressive worsening of the predictive quality of all options (except for that of Chexal-Lellouche) as the flowrate and pressure are reduced. Below a mass flux of 10 kg/m^{2}s, and a pressure of 20 bar, even the best option (i.e. that of Chexal-Lellouche) started to exhibit a systematic over-prediction of the void. At flowrates lower that 20 kg/m^{2}s, and a pressure below 3 bar, RETRAN-3D failed to reach a converged solution. This suggests that the Chexal-Lellouche model is the optimum void model available in RETRAN-3D.

The code-to-code comparisons between RETRAN-3D, CORETRAN-01/VIPRE-02 and TRAC-BF1, and their assessment against NUPEC experimental subcooled and saturated void data, showed that, generally, there is acceptable agreement between the codes, except for a substantial discrepancy between the RETRAN-3D 5-equation model and VIPRE-02 for the subcooled void. All codes tend to over-predict the subcooled void, and to under-predict the saturated void. The RETRAN homogeneous flow option suggests that the slip ratio is smaller than 1.0 under these conditions, which is consistent with the experimental observations that the void concentrates at the wall. At intermediate pressures (between 50 and 100 bar), the saturated voids were well predicted, while acceptable agreements were obtained for the subcooled conditions; the 5-equation option in RETRAN-3D consistently over-predicted the void.

At the subchannel level, VIPRE-02 results showed that, in the presence of strong power-to-flow variations across an assembly, the code under-predicted the void fraction substantially, as for example in the vicinity of water rods and part-length rods. This limitation was attributed to the absence of a lateral void drift model in the code. Also, as mentioned earlier, the lack of models for the effect of the spacer grids on (i) local mixing, and (ii) entrainment in the annular flow regime, also needs to be noted. The overall conclusion is that the system code RETRAN-3D, as well as the core and subchannel code CORETRAN-01/VIPRE-02, give a generally good prediction of the void fraction.

8 REFERENCES

[1] C.E. Peterson, J.H. McFadden, M.P. Paulsen, G.C. Gose, and J.G. Shafford, *"ETRAN-3D - A Program for Transient Thermal-Hydraulic Analysis of Complex Fluid-Flow Systems, Volume 1: Theory and Numerics* Manual", EPRI NP-7450, Electric Power Institute (1996).

[2] L.D. Eisenhart, A.F. Dias, J.L. Westacot, T.J. Downar, and H.G. Joo, *"CORETRAN-01, Volume 1: Theory and Numerical Analysis"*, WO-3574, Electric Power Institute (1997).

[3] J.M. Kelly, C.W. Stewart, and J.M. Cuta, *"VIPRE-02: A Two-Fluid Thermal-Hydraulic Code for Reactor Core and Vessel Analysis: A Mathematical Modeling and Solution Methods"*, Nuclear Technology, Vol. 100, p. 246 (1992).

[4] N. Zuber and J.A. Findlay, *"Average Volumetric Concentration in Two-Phase Flow Systems"*, J. of Heat Tansfer, Vol. 87, pp. 453-468 (1965).

[5] G.B. Wallis, *"One-dimensional Two-Phase Flow"*, McGraw-Hill Book Company, New York, USA (1969).

[6] D. Maier and P. Coddington, *"Review of a Wide ange Void Correlation Against an Extensive Database of Void Measurements"*, 5th International Conference on Nuclear Engineering, Paper No 2434, Nice, France, May 26-30, 1997.

[7] K.G. Pearson and M.K. Denham, *"Achilles Unballooned Cluster Experiments, Part 4: Low Pressure Level Swell Experiments"*, AEEW-R 2339, United Kingdom Atomic Energy Authority, Winfrith Technology Centre, Safety and Engineering Science Division, Winfrith (1989).

[8] D. Jowitt, C.A. Cooper, and K.G. Pearson, *"The THETIS 80% Blocked Cluster Experiment, Part 5: Level Swell Experiments"*, AEEW-R 1767, AEE Winfrith, Safety and Engineering Science Division, Winfrith (1984).

[9] R. Deruaz, P. Clement, and J.M. Veteau, *"Study of Two-dimensional Effects in the Core of a Light Water Reactor During the ECC's Phase Following a Loss of Coolant Accident"*, EUR 10076 EN, Commissariat a l'Energie Atomique, Centre d' Etudes Nucleaires de Grenoble, Service des Transferts Thermiques, Grenoble (1985).

[10] J. Dreier, G. Analytis, and R. Chawla, *"NEPTUN-III Reflooding and Boiloff Experiments with an LWHCR Fuel Bundle Simulator: Experimental Results and Initial Code Assessment Efforts"*, Nuclear Technology, Vol. 80, pp. 93-106 (1988).

[11] T. Mitsutake, S. Morooka, K. Suzuki, S. Tsunoyama, and K. Yoshimura, *"Void Fraction Estimation Within Rod Bundles Based on Three-Fluid Model and Comparison with X-Ray CT Void Data"*, Nuclear Engineering and Design, Vol. 120, pp. 203-212 (1990).

[12] S. Morooka, A. Inoue, M. Oishi, T. Aoki, K. Nagaoka, and H. Yoshida, *"In-Bundle Void Measurement of BWR Fuel Assembly by X-Ray CT Scanner"*, ICONE-1 Proceedings, pp. 237-243 (1991).

[13] Y. Anoda, Y. Kukita, and K. Tasaka, *"Void Fraction Distribution in Rod Bundle under High Pressure Conditions"*, Proceedings of the ASME Winter Annual Meeting, Advances in Gas-Liquid Flows, pp. 283-289 (1990).

[14] H. Kumamaru, M. Kondo, H. Murata, and Y. Kukita, 1994, *"Void-fraction Distribution under High-pressure Boil-off Conditions in Rod Bundle Geometry"*, Nuclear Engineering and Design, Vol. 150, pp. 95-105 (1994).

[15] T.M. Anklam, and R.F. Miller, *"Void Fraction under High Pressure, Low Flow Conditions in Rod Bundle Geometry"*, Nuclear Engineering and Design, Vol. 75, pp. 99-105 (1982).

[16] M. Ishii, *"One-Dimensional Drift Flux Model and Constitutive Equations for Relative Motion Between Phases in Various Two-Phase Flow Regimes"*, ANL-77-47 (1977).

[17] G.C. Gardner, *"Fractional Vapour Content of a Liquid Pool through which Vapour is Bubbled"*, Int. Journal of Multiphase Flow, Vol. 6, pp. 399-410 (1980).

[18] L-H. Liao, A. Parlo, and P. Griffiths, *"Heat Transfer, Carryover and Fall Back in PWR Steam Generators during Transients"*, NUREG/CR-4376, EPRI NP-4298, Sept. 1985.

[19] K. Takeuchi, M.Y. Young, and L.E. Hochreiter, *"Generalized Drift Flux Correlation for Vertical Flow"*, Nuclear Science and Engineering, Vol. 112, pp. 170-180 (1992).

[20] K.H. Sun, R.B. Duffey, and C.M. Peng, *"A Thermal-Hydraulic Analysis of Core Uncovery"*, Proceedings of the 19th National Heat Transfer Conference, Experimental and Analytical Modeling of LWR safety experiments, pp. 1-10 (1980).

[21] H.G. Sonnenburg, *"Full-Range Drift-Flux Model Base on the Combination of Drift-Flux Theory with Envelope Theory"*, NURETH-4 Proceedings, Vol. 2, pp. 1003-1009 (1989).

[22] S. Morooka, T. Ishizuka, M Iizuka, and K. Yoshimura, *"Experimental Study on Void Fraction in a Simulated BWR Assembly (Evaluation of Cross-Sectional Averaged Void Fraction)"*, Nuclear Engineering and Design, Vol. 114, pp. 91-98 (1989).

[23] G.E. Dix, *"Vapor Void Fractions for Forced Convection with Subcooled Boiling at Low Flow Rates"*, NEDO-10491, November 1971.

[24] D. Bestion, 1990, *"The Physical Closure Laws in the CATHARE Code"*, Nuclear Engineering and Design, Vol. 124, pp. 229-245 (1990).

[25] B. Chexal, J. Horowitz, and G. Lellouche, *"An Assessment of Eight Void Fraction Models for Vertical Flows"*, NSAC-107, Electric Power Research Institute, Nuclear Safety Analysis Center, Palo Alto (1989).

[26] A. Inoue, T. Kurosu, M. Yagi, S. Morooka, A. Hoshide, T. Ishizuka, and K. Yoshimura, *"In-Bundle Void Measurement of a BWR Fuel Assembly by an X-Ray CT Scanner: Assessment of BWR Design Void Correlation and Development of New Void Correlation"*, Proceedings of the ASME/JSME Nuclear Engineering Conference, Vol. 1, pp. 39-45 (1993).

[27] C.W. Stewart, J.M. Cuta, S.D. Montgomery, J.M. Kelly, K.L. Basehore, T.L. George, and D.S. Rowe, *"VIPRE-01: A Thermal-Hydraulic Analysis Code for Reactor Cores, Volume 1: Mathematical Modeling"*, EPRI NP-2511-CCM, Electric Power Institute (1993).

[28] D. Maier, P. Coddington, "Evaluation of the Slip Options in RETRAN-3D", 9th International RETRAN Meeting, Monterey, California, June 7-10, 1998.

[29] D. Maier and P. Coddington, *"Assessment of the Slip Options in RETRAN-3D against a Wide Range of Rod Bundle Void Data"*, 6th International Conference on Nuclear Engineering, Paper ICONE-6161, San Diego, California, USA, May 10-15, 1998.

[30] G.S. Lellouche and B.A. Zollotar, *"Mechanistic Model for Predicting Two-Phase Void Fraction for Water in Vertical Tubes, Channels, and Rod Bundles"*, NP-2246-SR, Electric Power Institute, February 1982.

[31] P. Coddington, Y. Aounallah, D. Maier, and D. Reedha, *"Assessment of the Subcooled Models in RETRAN-3D, VIPRE-02 and TRAC-BF1"* , 9th International Topical Meeting on Nuclear Thermal Hydraulics, San Francisco, California, October 3-8, 1999.

[32] Y. Anoda, Y. Kukita, and K. Tasaka, *"Void Fraction Distribution in Rod Bundle under High Pressure Conditions"*, Proceedings, ASME Winter Annual Meeting, Advances in Gas-Liquid Flows, pp. 283-289 (1990).

[33] K. Hori, Y. Akiyama, K. Miyazaki, H. Nishioka, and N. Tadeka, *"Total Evaluation of in Bundle Void Fraction Measurement Test of PWR Fuel Assembly"*, Int. Conf. on Nucl. Engineering, Volume 1 - Part B, ASME, p. 801-811 (1996).

[34] K. Hori, Y. Akiyama, K. Miyazaki, H. Kurosu, and S. Sugiyama, *"Void Fraction in a Single Channel Simulating One Subchannel of a PWR Fuel Assemby"*, Proc. First Int. Symposium on Two-Phase Flow Modelling and Experimentation, Rome, Italy, October 9-11, pp. 1013-1027 (1995).

[35] Y. Aounallah and P. Coddington, "*VIPRE-02 Subchannel Validation Against NUPEC BWR Void Fraction Data"*, Nuclear Technology, **128**, p. 225 (1999).

[36] Y. Aounallah and P. Coddington, *"Assessment of VIPRE-02 Void Fraction Prediction Against NUPEC Experimental Data"*, 9th International Topical Meeting on Nuclear Thermal Hydraulics, San Francisco, California, October 3-8, 1999.

[37] A. Inoue, M. Futakuchi, M. Yagi, T. Kurosu, T. Mitsutake, and S. Morooka, *"Void Fraction Distribution in a Boiling Water Reactor Fuel Assembly and the Evaluation of Subchannel Analysis Codes"*, Nuclear Technology, **112**, 3 (1995).

[38] A. Inoue, T. Kurosu, T. Oaki, M. Yagi, T. Mitsutake, and S. Morooka, *"Void Fraction Distribution in Boiling Water Reactor Fuel Assembly and Evaluation of Subchannel Code"*, J. of Nuclear Science and Technology, **32**, 7 (1995).

[39] M. Yagi, T. Mitsutake, S. Morooka, and A. Inoue, *"Void Fraction Distribution in BWR Fuel Assembly and the Evaluation of Subchannel Code"*, Paper in Subchannel Analysis in Nuclear Reactor, p. 141, Edited by H. Ninokata and M. Aritomi, Institute of Applied Energy and the Atomic Energy Society of Japan (1992).

[40] S. Morooka, A. Inoue, M. Oishi, T. Aoki, K. Nagaoka, and H. Yoshida, *"In-bundle Void Measurement of BWR Fuel Assembly by X-ray CT Scanner"*, Proc. The 1st JSME-ASME Joint International Conference on Nuclear Engineering, Tokyo, Japan Society of Mechanical Engineers, p. 237 (1991).

[41] G. Yadigaroglu and A. Magnas, *"Equilibrium Quality and Mass Flux Distribution in an Adiabatic Three-Subchannel Test Section"*, Nuclear Technology, **112**, p. 359 (1995).

[42] R.T. Lahey and F.J. Moody, *"The Thermal-Hydraulics of a Boiling Water Nuclear Reactor"*, 2nd ed., p. 74, American Nuclear Society, Illinois, (1993).